PHYSICAL REVIEW C VOLUME 35, NUMBER 5 MAY 1987

Heavy-ion collision theory with momentum-dependent interactions

C. Gale
Physics Department, University of Minnesota, Minneapolis, Minnesota 55455

G. Bertsch
Physics Department and Cyclotron Laboratory, Michigan State University, East Lansing, Michigan 48824

S. Das Gupta
Department of Physics, McGill University, Montreal, Quebec, Canada
(Received 29 October 1986)

We examine the influence of momentum-dependent interactions on the momentum flow in 400 MeV/nucleon heavy ion collisions. Choosing the strength of the momentum dependence to produce an effective mass $m^*=0.7m$ at the Fermi surface, we find that the characteristics of a stiff equation of state can be obtained with a much softer compressibility.

INTRODUCTION

A major goal in the study of intermediate energy heavy ion collisions is to measure the equation of state of nuclear matter. The observable that shows most promise for this measurement is the momentum flow in the collision. It can be analyzed by the sphericity of the final state momentum distribution,[1] or by the transverse momentum within an inferred reaction plane.[2] At present, the best founded theory for interpreting the experiments is based on the Boltzmann equation, including a self-consistent potential field and a collision integral of the Uehling-Uhlenbeck form. We developed a technique for numerically solving the Boltzmann-Uehling-Uhlenbeck (BUU) equation,[3] and it has been successfully applied to momentum flow and its dependence on the assumed equation of state.[4,5]

The equation of state enters the theory via the functional dependence of the mean field potential on the particle density in phase space. In the above-quoted studies the potential was assumed to depend only on the ordinary density, ignoring the well-known momentum dependence of the field. For example, the attractive potential as seen in nucleon scattering from nuclei weakens and becomes small when the nucleon has an energy of a few hundred MeV.[6] In theoretical potentials based on Brueckner theory, the momentum dependence gives the particles near the Fermi surface an effective mass in the range $m^*/m=0.6$–0.7. The overall interaction will be more repulsive under the conditions of the heavy ion collision if this momentum dependence is included in the BUU equation. Thus the effects of a stiff equation of state may occur with a softer model.[7] Physically, there are two mechanisms at work here. The average momentum of a particle in the medium is higher in a heavy ion collision than for cold nuclear matter at the same density; the repulsive character of the momentum dependence implies that the potential field will be shallower. Also, particles will move with a higher velocity for a given momentum than in free space, transporting momentum more effectively from one part of the system to another.

In this work we shall examine quantitatively the above effects using a phenomenological model of the momentum dependence. Momentum dependent interactions have been applied previously to studies of momentum flow,[8,9] but only in mean-field theory, which is unrealistic at high energy. Our model and some general considerations are discussed in the following section. The section following that describes our numerical study of the model.

MOMENTUM-DEPENDENT MEAN FIELDS

It is essential that a theory of momentum transport respect the conservation laws. This will be guaranteed if the dynamic equations are derived from an energy functional. We assume the existence of such a functional and call its interaction part W. Its derivative with respect to density is the single particle potential,

$$U(\rho,p)=\frac{\delta W}{\delta \rho_p} . \tag{1}$$

In previous work, we chose U as a sum of powers of ρ, omitting any p dependence. We now introduce an additional p-dependent term. The main origin of the p dependence in Brueckner theory is the nonlocality of the exchange interaction. This interaction is attractive and important at low momentum, but it weakens and disappears at very high momentum. The function of momentum describing meson exchange interactions has these properties, and we adopt that parametrization,

$$U(\mathbf{p})\sim\frac{1}{1+(\mathbf{p}-\langle\mathbf{p}'\rangle)^2/\Lambda^2} .$$

Here $\mathbf{p}$ is the momentum of the particle, and Λ is a scale parameter. Translational invariance is preserved by measuring $\mathbf{p}$ with respect to $\langle\mathbf{p}'\rangle$, the average momentum of the other particles in the neighborhood. The density dependence of this potential will be taken appropriately for a two-body interaction, i.e., a linear dependence on ρ. To make the model definite, we arbitrarily choose the

momentum scale $\Lambda=400$ MeV/c, and adjust the strength of the potential to make the effective mass satisfy $m^*/m=0.7$ at the Fermi surface for ordinary nuclear matter density. This condition implies

$$\left.\frac{dU(\rho_0,p)}{dp}\right|_{p_F}=\frac{0.43}{m}\ ;$$

the resulting p-dependent potential is given by

$$U_p=\frac{c\rho/\rho_0}{1+\left[\frac{\mathbf{p}}{\Lambda}\right]^2},\quad c=-75\text{ MeV},\quad \Lambda=1.5p_F\ . \tag{2}$$

The requirement that U be derivable from an energy functional can be met by taking the p-dependent part of the interaction energy to have the form

$$W_p=\int d\mathbf{r}\sum_{\mathbf{p},\mathbf{p}'}\frac{f(\mathbf{p},\mathbf{r})f(\mathbf{p}',\mathbf{r})c/\rho_0}{1+\left[\frac{\mathbf{p}-\langle\mathbf{p}'\rangle)}{\Lambda}\right]^2}\ . \tag{3}$$

Here $f(\mathbf{p},\mathbf{r})$ is the nucleon density in phase space. Applying Eq. (1) to determine U, we find two terms, one being Eq. (2) and the other given by

$$U'=c\frac{\rho}{\rho_0}\left\langle\frac{1}{1+\left[\frac{\mathbf{p}'}{\Lambda}\right]^2}\right\rangle\ . \tag{4}$$

The expectation value in Eq. (4) is over the momentum of the particles in the medium; it does not depend on the momentum of the particle under consideration. The term (4) was omitted in an earlier version of this work,[12] giving less effect of the momentum dependence.

We complete the model as in the previous studies by adding an ordinary two-body potential and a density-dependent potential. Additional parameters are constrained by the values of the density and binding energy of nuclear matter at saturation. One parameter, the power of the density dependence, is left free to vary the equation of state. The full expression for the potential field is

$$U(\rho,\mathbf{p})=+a\rho/\rho_0+b(\rho/\rho_0)^\sigma+\frac{c\rho/\rho_0}{1+(\mathbf{p}-\langle\mathbf{p}'\rangle)^2/\Lambda^2}+\frac{c\rho}{\rho_0}\left\langle\frac{1}{1+\left[\frac{\mathbf{p}'}{\Lambda}\right]^2}\right\rangle\ . \tag{5}$$

The corresponding potential energy density is

$$W(\rho)=+\frac{a}{2}\frac{\rho^2}{\rho_0}+\frac{b}{1+\sigma}\left[\frac{\rho}{\rho_0}\right]^\sigma\rho+\frac{c\rho^2}{\rho_0}\left\langle\frac{1}{1+\left[\frac{\mathbf{p}'}{\Lambda}\right]^2}\right\rangle\ . \tag{6}$$

For our momentum-dependent model we use $\sigma=\frac{7}{6}$, and obtain the other parameters by requiring nuclear matter saturation at $E=-16$ MeV and $p_F=1.34$ fm^{-1}. We call this the lightweight model, to distinguish it from the models with mass $m^*=m$ introduced earlier. The parameters for the lightweight, the soft, and the stiff models are quoted in Table I.

To understand the differences in dynamics arising in these models it is helpful to analyze the momentum transport. A conserved momentum current $\Pi_{\mu\nu}$ may be defined when the energy functional depends only on the local phase space density. The conserved current satisfies the equation of continuity,

$$\frac{d\,\mathbf{p}(\mathbf{r})}{dt}+\nabla\cdot\tilde{\Pi}(\mathbf{r})=0\ , \tag{7}$$

where $\mathbf{p}(\mathbf{r})$ is the momentum density at $\mathbf{r}$. The momentum current consists of two terms, contributing via the particle current and from the potential field. The particle part is given by

$$\Pi_{\mu\nu}^{\text{particle}}=\sum_p(v^{\text{free}}+\nabla_p U)_\mu p_\nu f(p,r)\ , \tag{8}$$

where the free velocity is

$$\mathbf{v}^{\text{free}}=\frac{\mathbf{p}}{(m^2+p^2)^{1/2}}$$

with relativistic kinematics. The potential field term is

$$\Pi_{\mu\nu}^{\text{field}}=\delta_{\mu\nu}(\rho U-W)\ . \tag{9}$$

For a cold system the distribution function is a Fermi sphere of radius p_F, and the pressure is given by the longitudinal momentum flux,

$$P=\Pi_{zz}=\frac{1}{5}\frac{p_F^2}{m}\rho+\frac{a}{2}\frac{\rho^2}{\rho_0}+\frac{\sigma}{\sigma+1}b\frac{\rho^{\sigma+1}}{\rho_0^\sigma}+\frac{c\rho^2/\rho_0}{1+p_F^2/\Lambda^2}\ . \tag{10}$$

For hot matter it is useful to express the pressure using as a variable the free particle kinetic energy (per particle), T. The formula is then

$$P=\tfrac{2}{3}T\rho-\tfrac{2}{3}c\frac{\rho^2}{\rho_0}\left\langle\frac{p'^2/\Lambda^2}{[1+(p'/\Lambda)^2]^2}\right\rangle_T+\frac{a}{2}\frac{\rho^2}{\rho_0}+\frac{\sigma}{1+\sigma}b\frac{\rho^{\sigma+1}}{(\rho_0)^\sigma}+\frac{c\rho^2}{\rho_0}\left\langle\frac{1}{1+(p'/\Lambda)^2}\right\rangle_T\ . \tag{11}$$

The single number used to characterize the momentum transport is the compressibility of the matter at saturation density. In nuclear physics the compressibility is conventionally defined as in Eq. (13) below. Fixed entropy transformations produce a scaling transformation of the $f(\mathbf{p})$, and the kinetic energy per particle varies as

$$T'=T\left[\frac{\rho'}{\rho}\right]^{2/3}\ . \tag{12}$$

The formula for the compressibility of cold matter at $\rho=\rho_0$ is

TABLE I. Potential model parameters for saturation at $p_F = 1.34$ fm^{-1} and binding energy of 16 MeV/nucleon. The first five columns quote the parameters in Eq. (5), and the last column gives the compressibility from Eq. (13).

Model	a (MeV)	b (MeV)	σ	c (MeV)	Λ (p_F)	K (MeV)
Lightweight	−144.9	203.3	$\frac{7}{6}$	−75	1.5	215
Soft	−358.1	304.8	$\frac{7}{6}$	0		201
Stiff	−123.6	70.4	2	0		377

$$K = \frac{9\partial P}{\partial \rho}\bigg|_s = 9\left[\frac{1}{3}\frac{p_F^2}{m} + a + b\sigma + \frac{2c}{1+\left[\frac{p_F}{\Lambda}\right]^2} - \tfrac{2}{3}c\left[\frac{p_F}{\Lambda}\right]^2\left[\frac{1}{1+\left[\frac{p_F}{\Lambda}\right]^2}\right]^2\right] . \quad (13)$$

In Table I we quote the values of the compressibility coefficient for the three models, calculated from Eq. (13). We see that the lightweight model behaves like the soft model near nuclear matter density. The question before us will be how closely it resembles the stiff model under the conditions of the heavy ion collision.

DYNAMICS OF CENTRAL COLLISIONS

Before proceeding with the numerical studies, we examine the behavior of the collision in the continuum limit, where classical shock dynamics applies. The density in the shocked region is determined from the conservation laws of particle number, momentum, and energy. The other variable besides the density to describe the shocked matter we take to be T. Then the equations for the matter are the following two implicit equations for ρ and T,

$$\frac{v_0 p_0}{\rho_s/\rho_0 - 1} = \Pi(\rho_s, T_s)/\rho_s , \quad (14a)$$

$$e = T_s + W(\rho_s, T_s)/\rho_s . \quad (14b)$$

Here ρ_s and T_s are the density and free kinetic energy in the shocked matter, v_0 is the velocity of the incoming matter, p_0 is its momentum per particle, and e is the energy per particle. We consider 400 MeV/nucleon heavy ion collisions, which gives in the c.m. system initial conditions $v_0 = 0.43c$, $p = 440$ MeV/c, and $e = 84$ MeV, taking into account the binding energy of the initial matter. The predicted shock conditions are shown in Table II. In Fig. 1, we show the equation of state for the models, starting from the shocked matter at ρ_s and T_s and expanding adiabatically according to Eq. (12). The lightweight model has a stiffer equation of state than the soft model, as expected from the qualitative arguments. The maximum density is lower, and the pressure at a given density is higher than in the soft model. However, the differences are rather small, and the lightweight model is closer to the soft than to the stiff model. Thus we expect not to see major differences in the physical observables between the soft and lightweight models, from the dynamics in local equilibrium.

To make a more detailed comparison between the arguments from the bulk behavior and the actual dynamics of the collision system, we shall examine the evolution of the central density in some detail. This is simply related to the pressure in the middle, if the system comes into local equilibrium. A simple argument can be made about the time history of the central pressure, based on momentum conservation. Given a rough knowledge of the initial and final states, we know how much momentum is transferred across the plane at longitudinal coordinate zero. This momentum transfer must equal the integral of the pressure over the plane and over time. The initial longitudinal momentum density in each half plane is just the initial momentum per nucleon times the areal density of nucleons. The final state is roughly isotropic in momentum space, so the longitudinal momentum density is about $-\frac{1}{2}$ of the initial, assuming we can neglect the transverse spread in the particle distribution. Thus we expect the momentum flux density to satisfy

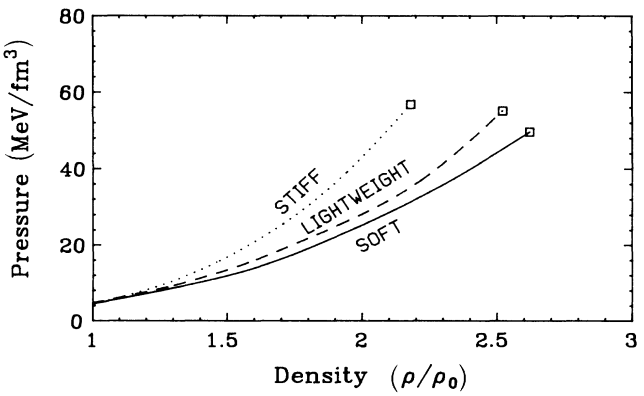

FIG. 1. Equation of state for the various models. The pressure is shown for the shocked matter from 400 MeV/nucleon collisions of slabs of nuclear matter. The initial shock conditions are determined from Eq. (14), and the subsequent expansion from Eqs. (11) and (12).

TABLE II. Shock conditions for 400 MeV/nucleon heavy ion collisions.

Model	ρ_s	T_s (MeV)	Π (MeV fm^{-3})
Soft	2.62	121.3	50
Lightweight	2.52	96.5	51
Stiff	2.18	108.3	57

$$(1+\tfrac{1}{2})p_0\rho_0 2R \approx \int dt\, \Pi_{zz}(\rho(t),T(t)) , \tag{15}$$

where $2R$ is the longitudinal dimension of one of the colliding nuclei. This integral can be expressed as an integration over the density achieved in the central region by defining a density duration function,

$$g(\rho')= \int dt\, \delta(\rho'-\rho(t)) . \tag{16}$$

Then the longitudinal momentum transfer density satisfies

$$\tfrac{3}{2}p_0\rho_0 2R \approx \int_0^{\rho_s} d\rho\, g(\rho)\Pi_{zz}(\rho,T(\rho)) . \tag{17}$$

NUMERICAL APPLICATION

We solve the BUU equation using test particles to represent the phase space density and the particle-in-cell method to treat the mean field, as in Ref. 3. Hamilton's equations of motion for the test particles are modified by the presence of the two new terms in the acceleration equation,

$$\dot{\mathbf{p}}= -\nabla U , \tag{18}$$

and by the presence of a field term in the velocity equation,

$$\dot{\mathbf{r}}= \frac{\mathbf{p}}{(m^2+p^2)^{1/2}} + \frac{dU}{d\mathbf{p}} . \tag{19}$$

Previously, the calculation required storing the phase space coordinates of the test particles and the density in a spatial grid of cells. The new calculation requires in addition the average momentum of the particles in a cell $\langle \mathbf{p}' \rangle$, and also the average of the function $1/[1+(\langle \mathbf{p}' \rangle)^2/\Lambda^2]$. These changes have practically no effect on the time it takes to do a calculation, since most of the time is consumed in treating the collision integral.

The nucleon-nucleon scattering is treated by a model of Cugnon *et al.*[6] This is a fit to the free scattering cross section, and includes pion production by a Δ resonance approximation.

On a numerical level, the calculation requires several additional parameters. One of these is the number of test particles to represent one physical particle, which we take to be 60. Thus the calculation of Nb + Nb collisions requires following about 11 000 test particles. Another parameter is the cell size for the potential calculation. We use cubic cells with a side of 1.5 fm. The arena size is 14 fm$\times$13 fm$\times$21 fm, requiring about 13 000 cells in all. Finally, the time step size was taken to be 0.5 fm/c.

We now discuss a representative set of runs for 400 MeV/nucleon Nb + Nb collisions, using the various potential models. Figure 2 shows the time history of the density for the three models, taken at a fixed impact parameter $b=2.1$ fm. This is the average impact parameter for the collisions which comprise the most central 7% of the reaction cross section. There are significant differences between the soft and stiff models, with the central density in the soft model rising to about 2.4 times nuclear matter density, compared to the predicted 2.6 of the bulk dynamics. The density in the stiff equation of state reaches only $2.0\rho_0$, compared to the expected 2.2. The initial density increase in the lightweight model is slower than for either of the others. This is because the particles are moving faster and the overlap zone is larger at a given time step. Eventually at middle times the density in the lightweight model is about halfway between the soft and stiff.

The next quantity we examine is the density duration function $g(\rho)$, which is plotted in Fig. 3. There is in each case a peak, whose position indicates the average density in the compressed phase. The area of the peak is proportional to the time duration of the compressed phase. We evaluated the momentum balance condition, Eq. (17), integrating the function $g(\rho)$ numerically with the pressure from Fig. 1. The results are shown in Table III. We see that the momentum balance fails by about 40%, with the bulk limit smaller than the actual momentum transfer. It should not be surprising that the actual momentum transfer is higher. For one thing, considerable time is required before the system reaches a local equilibrium. Be-

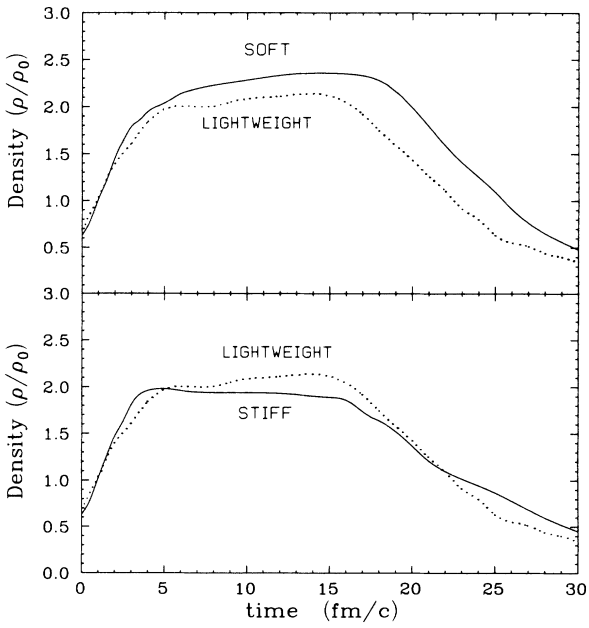

FIG. 2. Central density in collisions of 400 MeV/nucleon Nb ions on an Nb target, at an impact parameter of 2.1 fm. The lightweight model, shown as the dotted curve, is compared with the soft model in the upper curve, and the stiff model below.

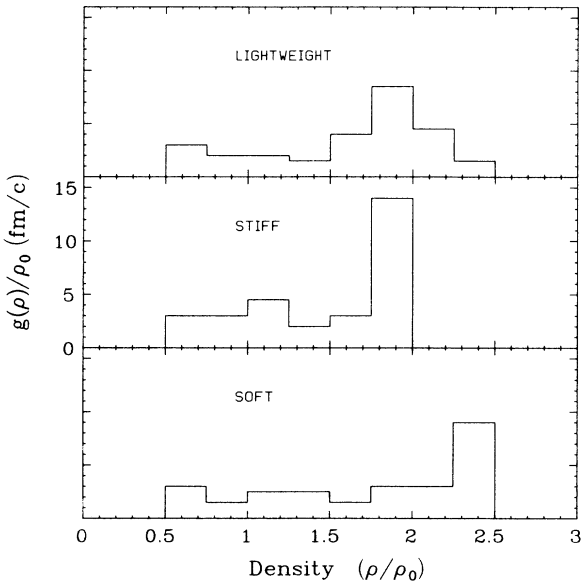

FIG. 3. Density duration function $g(\rho)$, defined in Eq. (16).

fore that, there is relatively more longitudinal momentum transfer due to the directed motion in the longitudinal direction. Also, to the extent that the system expands laterally, the effective areal density of nucleons is smaller than assumed in Eq. (17). Note that the balance fails more for the lightweight model than the others. The particle momentum transport in the initial phase is more effective with the faster moving particles.

The equilibration rate and speed of energy transport can have important influences on the transverse momentum. Transverse momentum is only generated effectively by the particle transport after the system comes into local equilibrium. The transverse momentum also depends on the transverse area of the system, and this will be larger if the equilibration takes place earlier when the system is still extended in the longitudinal direction. The collision rate tends to decrease with increasing stiffness, but the lightweight model has a larger collision rate than the soft model for the first 15 fm/c.

We now examine the observables related to transverse momentum. The transverse momentum, as a function of longitudinal velocity in the final state, is plotted in Fig. 4, using the Danielewicz-Odyniec analysis technique to infer the reaction plane from individual collision events. The results show a significant difference between soft and stiff models. This is easily understood from considerations of bulk dynamics. The relevant quantity is the total momentum transferred across a plane perpendicular to the reaction plane. The integral is similar to the one for the longitudinal momentum density, except for an additional integration over area. The result would be independent of the model, as in the longitudinal case, if the areas were the same. However, the transverse area should scale as the inverse of the central density, so the models producing higher density should have smaller transverse momentum generated. The equilibration goes in the other direction, with the stiff model taking longer and producing less

TABLE III. Longitudinal momentum balance.

Equation (17), lhs	1000 MeV c fm^2
Equation (17), rhs	
Soft	680 MeV c fm^2
Lightweight	540 MeV c fm^2
Stiff	670 MeV c fm^2

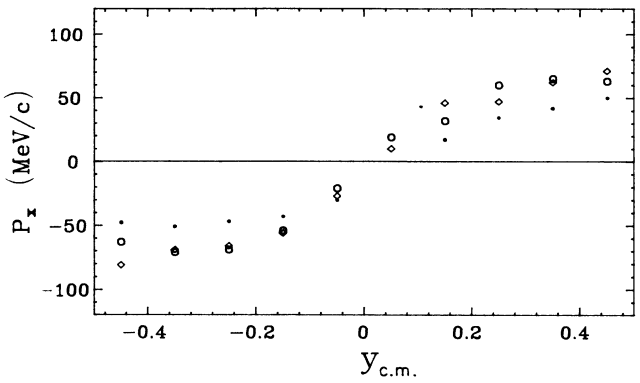

FIG. 4. Transverse momentum generated in the collision. Results are averaged over impact parameters between 0 and 3 fm. The predictions of the soft, the stiff, and the lightweight models are shown as points, circles, and diamonds, respectively.

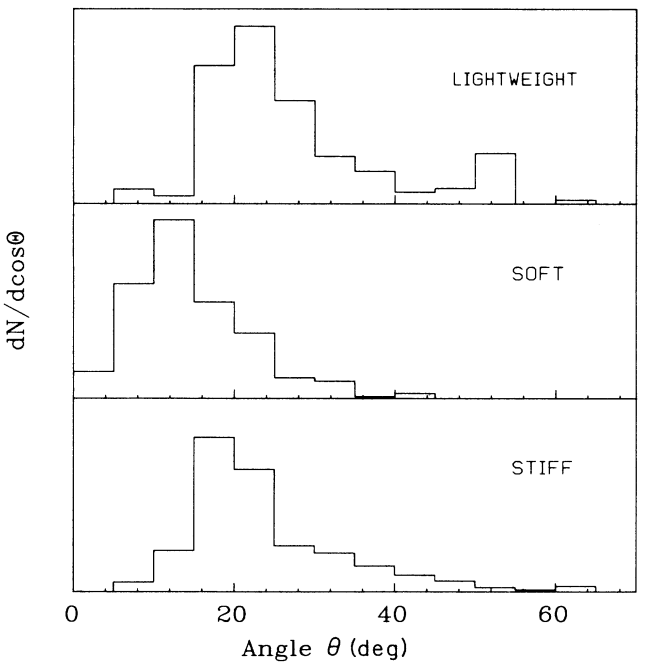

FIG. 5. Flow angle for the Nb + Nb collision. The three histograms show the results from the lightweight, the soft, and the stiff models, going from top to bottom.

transverse momentum at early times. From these arguments we see why effects are small. The lightweight model achieves a stiffer equation of state with a rapid equilibration rate, and so can produce as much transverse momentum as the stiff model. Finally, we also show the flow angle comparisons in Fig. 5, which behave in a similar way. The flow angle distribution for the lightweight model is close to the measurement of Ref. 1.

From comparison of the momentum-independent models with the data, it has been concluded that the equation of state is rather stiff.[4] Our results show that a soft equation of state can produce the same results when a reasonable momentum dependence is included in the model. A significant factor is the equilibration rate, and this points to the need to study the NN collisional model more closely. Studies at lower energies show a sensitivity of polarizations to the assumed NN cross section;[10] the dependence of observables on the NN cross section needs to be further explored in the intermediate energy regime.

In this work we have not attempted to compare the transverse momentum distribution directly with data. The plots in Fig. 4 show flat plateaus changing rapidly at the midvelocity point. In contrast, the experimental data show a smooth, almost linear variation of transverse momentum with longitudinal velocity.[11] The smoothness may be due largely to the limitations of the detector apparatus. The authors of Ref. 11 recommend making comparison after filtering the theoretical predictions with a computer program that simulates the experimental detection conditions. However, we feel that we need to understand the detector filtering better in order to draw conclusions from distributions that look quite different before and after the filtering process.

ACKNOWLEDGMENTS

Conversations with V. Pandharipande and P. Siemens which led to this study are gratefully acknowledged. We further benefitted from conversations with U. Mosel and L. Csernai. We acknowledge grants from the Minnesota Supercomputer Center and the McGill Computer Center, where the numerical work was done. This work was supported by the National Science Foundation under Grant no. PHY 85-19653, by the Natural Sciences and Engineering Research Council of Canada, by the Quebec Department of Education, and by the School of Physics and Astronomy of the University of Minnesota.

[1]H. A. Gustafsson *et al.*, Phys. Rev. Lett. **52**, 1590 (1984).
[2]P. Danielewicz and G. Odyniec, Phys. Lett. **157B**, 146 (1985).
[3]G. Bertsch, H. Kruse, and S. Das Gupta, Phys. Rev. C **29**, 673 (1984); **33**, 1107(E) (1986).
[4]H. Kruse, B. V. Jacak, and H. Stoecker, Phys. Rev. Lett. **54**, 289 (1985).
[5]S. Das Gupta, in *Proceedings of the International Conference on Nuclear Physics, Bombay, 1984,* edited by B. K. Jain and B. C. Sinha (World-Scientific, Singapore, 1985), p. 70.
[6]J. Cugnon, T. Mizutani, and J. Vandermeulen, Nucl. Phys. **A352**, 505 (1981).
[7]V. Pandharipande and P. Siemens, private communication.
[8]B. Schürmann and W. Zwermann, Phys. Lett. **158B**, 366 (1985).
[9]R. Y. Cusson *et al.*, Phys. Rev. Lett. **55**, 2786 (1985).
[10]M. B. Tsang *et al.*, Phys. Rev. Lett. **57**, 559 (1986).
[11]K. Doss *et al.*, Phys. Rev. Lett. **57**, 302 (1986).
[12]Workshop on Nuclear Equation of State, Berkeley, 1986.